Cancer Science
Japanese Cancer Association JCA
Open Access

# Early hepatocellular carcinoma with high-grade atypia in small vaguely nodular lesions

Hidenori Ojima,[1] Yohei Masugi,[1] Hanako Tsujikawa,[1] Katsura Emoto,[1] Yoko Fujii-Nishimura,[1] Mami Hatano,[1] Miho Kawaida,[1] Osamu Itano,[2] Yuko Kitagawa[2] and Michiie Sakamoto[1]

[1]Departments of Pathology; [2]Surgery, Keio University School of Medicine, Tokyo, Japan

**Key words**

Cyclase-associated protein 2, early hepatocellular carcinoma, high grade, scirrhous component, stromal invasion

**Correspondence**

Michiie Sakamoto, Department of Pathology, Keio University School of Medicine, 35 Shinanomachi, Shinjuku-ku, Tokyo 160-8582, Japan.
Tel: +81-3-5363-3762; Fax: +81-3-3353-3290;
E-mail: msakamot@z5.keio.jp

**Funding Information**

This study was supported by a Grant-in-Aid for Scientific Research B from the Ministry of Education, Culture, Sports, Science and Technology of Japan and a Health Labour Sciences Research Grant from the Ministry of Health, Labour and Welfare of Japan.

Received October 8, 2015; Revised December 31, 2015; Accepted January 14, 2016

*Cancer Sci* **107** (2016) 543–550

doi: 10.1111/cas.12893

**Multistep hepatocarcinogenesis progresses from dysplastic nodules to early hepatocellular carcinoma (eHCC) and to advanced HCC. The aim of the present study was to investigate the detailed histopathological features of eHCC. We investigated 66 small vaguely nodular lesions resected from 40 patients. The degree of cellular and structural atypia and stromal invasion were assessed. The immunohistochemical expression of HCC-related markers adenylate cyclase-associated protein 2 (CAP2), heat shock protein 70 (HSP70), Bmi-1, CD34 and h-caldesmon were evaluated. Of the 66 nodules, 10 were diagnosed as low-grade dysplastic nodules (LGDN), 10 as high-grade dysplastic nodules (HGDN) and 46 as eHCC. Among the 46 eHCC, 18 nodules (39.1%) showed marked stromal invasion and/or the presence of the scirrhous component and were subclassified as high-grade eHCC (HGeHCC). The remaining 28 eHCC, which lacked these features, were subclassified as low-grade eHCC (LGeHCC) and were examined further. HGeHCC showed high levels of cellular and structural atypia and large tumor size. The immunohistochemical expression of CAP2 and the area of sinusoidal vascularization showed increases from LGDN to HGeHCC. The density of arterial tumor vessels was high in HGeHCC compared with other nodule types. Cluster analysis of these parameters subclassified 65 nodules into HGeHCC-dominant, LGeHCC and HGDN-dominant, and LGDN-dominant groups. These results indicate the increased malignant potential of HGeHCC and suggest that it is already a transitional stage to advanced HCC. We consider that our grading classification system may be valuable for considering treatment strategies for eHCC around 2 cm in diameter.**

Multistep hepatocarcinogenesis is characterized by the following three phases: premalignant dysplastic nodules (DN) (low grade or high grade), early hepatocellular carcinoma (eHCC) and finally advanced HCC.[1–4] Histopathologic diagnosis of these three types of lesions was established by an international consensus in 2009 and was also described in the 4th edition of the World Health Organization (WHO) classification in 2010.[5,6] Imaging diagnosis of these lesions also supports the presence of premalignant or early malignant lesions without definite features of advanced HCC that can transition to advanced HCC during follow up. In particular, hemodynamic changes detected by contrast-enhanced computed tomography or ultrasonography and hepatocellular changes detected by gadolinium ethoxybenzyl diethylene triamine pentaacetic acid-enhanced magnetic resonance imaging are useful for evaluating the malignant potential of these lesions.[7,8] Clinically, equivocal lesions smaller than 2 cm without definite features of HCC are frequently encountered in high-risk patients, such as those with chronic hepatitis and liver cirrhosis, and are generally followed up without treatment. Follow up of these nodules has revealed various possible changes, from disappearance or stability without change of nodule size or hemodynamics to increased nodule size and blood supply; that is, hypervascularization of the nodule.[8–10] It is hypothesized that equivocal nodules on imaging diagnosis include regenerative nodules, dysplastic nodules (DN) and eHCC; however, the clinical behavior of these nodules is quite heterogeneous, and, in particular, clinical diagnosis of eHCC is difficult.

Early hepatocellular carcinoma (eHCC) is characterized by an increased cell density, cellular and structural atypia, decreased intratumoral portal tracts, and the presence of variable numbers of unpaired arteries. In addition, stromal invasion is frequently observed; indeed, the presence of stromal invasion is one of the pathological features used to make a diagnosis of HCC.[5] Together with these histological features, a panel of immunohistochemical markers is reportedly useful in making a diagnosis of eHCC. These molecular markers include heat shock protein 70 (HSP70)[11] glypican-3, glutamine synthetase,[12] adenylate cyclase-associated protein 2 (CAP2)[13] and the polycomb gene product Bmi-1.[14] Most published studies have focused on the differential diagnosis of eHCC from DN; however, a detailed histopathological study of eHCC itself has not yet been conducted.

The aim of the current study was to investigate the detailed histopathological features of eHCC. Consequently, we conducted immunohistochemical analyses of vascular changes

and the expression of various molecular markers and conducted a detailed histopathological evaluation of the degree of cellular atypia, structural atypia and stromal invasion in 66 resected samples of small vaguely nodular type lesions.

## Materials and Methods

**Patients.** From 40 patients who underwent hepatectomy at Keio University Hospital from 1990 to 2013, 66 nodules smaller than 25 mm in diameter that showed as small vaguely nodular lesions macroscopically and were pathologically diagnosed at the time as DN or eHCC were selected for this study from pathological records. The nodule sizes ranged from 5 to 25 mm, with a mean value of 11.1 mm and a median value of 10 mm. The patients were 34 men and 6 women aged between 46 and 79 years (mean age: 62.6 years; median age: 60 years.) Operative indications were tumor resection in 21 patients and living donor liver transplantation in 19 patients. The patient backgrounds are summarized in Table S1. This study was approved by the institutional review boards of Keio University School of Medicine.

**Pathological analysis.** All histological diagnoses and evaluations of immunohistochemical stainings were conducted by two pathologists (H.O. and Y.M.) without reference to clinicopathological data. If the initial evaluation provided different results, a consensus interpretation was reached after re-examination.

**Histological diagnosis.** Nodular lesions were re-diagnosed as low-grade dysplastic nodules (LGDN), high-grade dysplastic nodules (HGDN), or eHCC based on the pathological diagnostic criteria of the WHO classification[6] and the international consensus classification.[5]

Using H&E-stained specimens, we observed and evaluated cellular atypia (size of the nucleus), structural atypia and tumor cell density throughout the whole tumor. Nuclear size (equal to/enlarged compared with non-tumoral liver tissue) and tumor cellularity (more than twofold/less than twofold compared with non-tumoral liver cellularity) were determined. Structural atypia was evaluated based on the presence of a scirrhous hepatocellular carcinoma-like pattern composed of fibrous stroma (denoting a "scirrhous component") in the lesion (Fig. 1a). Stromal (portal area) invasion was evaluated in elastic Van Gieson-stained sections. The extent of tumor invasion was evaluated according to the following four grades with reference to the elastic fiber seen in the outer circumference around the portal area: None, invasion was not found or was unclear; Suspected invasion, tumor cells were observed on the border part of the elastic fiber; Distinct invasion/mild, despite distinct invasion of the stroma in the portal area, further severe invasion was not found; Distinct invasion/severe, massive invasion (Fig. 1b,c) or invasion enclosing the portal vein and periphery of bile duct, invasion in an "Indian file pattern," or hepatic vein wall invasion (Fig. 1d–f).

**Immunohistochemical analysis.** Formalin-fixed, paraffin-embedded serial tissue sections 4-μm thick were placed on silane-coated slides for immunohistochemical analysis. The sections were deparaffinized, rehydrated in xylene and grade-diluted ethanol (50–100%), and then immersed for 20 min in

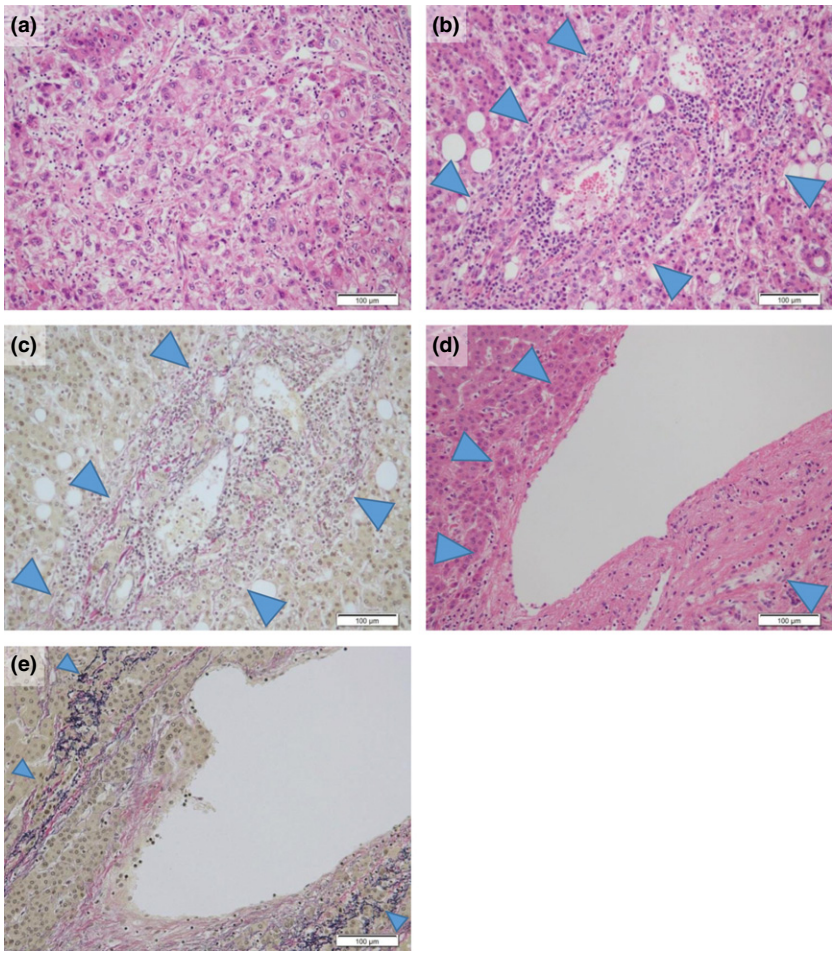


**Fig. 1.** Histopathological findings of structural atypia and severe distinct invasion. A scirrhous hepatocellular carcinoma-like pattern (scirrhous component) composed of rich fibrous stroma was seen in a case with structural atypia (a). In cases with severe distinct invasion, tumor cells showed massive portal area invasion (arrowheads) (b,c) and hepatic vein wall invasion (arrowheads) (d,e). (a,b, d) H&E stain; (c,e) elastic Van Gieson stain; scale bars = 100 μm.

0.3% hydrogen peroxide in absolute methanol to block endogenous peroxidase activity. Immunohistochemical staining using mouse anti-human HSP70 monoclonal antibody (1:500 dilution; SC-24; SantaCruz Biotechnology, Santa Cruz, CA, USA), mouse anti-human CD34 monoclonal antibody (1:50 dilution; QBEnd-10; Dako, Glostrup, Denmark) and mouse anti-human h-caldesmon monoclonal antibody (1:100 dilution; hCD; Dako) was performed using a Leica Bond-Max automated immunostainer (Leica Microsystems, Bannockburn, IL, USA). For CAP2 and Bmi-1, the tissue sections were heated at 120°C in 0.01 mol/L sodium citrate buffer, pH 7.0, for 10 min before incubation with rabbit anti-human CAP2 polyclonal antibody (1:4000 dilution) and mouse anti-human Bmi-1 polyclonal antibody (1:200 dilution; Upstate Biotechnology, Lake Placid, NY, USA), and immunohistochemical staining was performed using the ImmPRESS system (Vector Laboratories, Burlingame, CA, USA).

For CAP2 and HSP70, tumor cells showing strong expression compared with non-tumoral liver were considered to be positive (Fig. 2a,b), and for Bmi-1, tumor cells showing clear dot-pattern staining were considered to be positive (Fig. 2c). Subsequently, for each molecular marker, the number of positive tumor cells was counted by random selection of three areas of the tumor, and the average positive rate was calculated for evaluation. For CD34, positive sinusoidal vascular architectural areas in the scirrhous component of the tumor and in the rest of the tumor (Fig. 2d) were counted separately. We determined each areal rate of CD34 in 10% increments. All values less than 10% were counted as 5%, because there are no completely negative cases in the liver parenchyma in general, and a detailed measurement of positive areas evaluated at 10% or less may be difficult. For h-caldesmon, the number of intratumoral positive vessels (arterial tumor vessels) in the non-scirrhous component was counted in 10 visual fields at ×200 magnification (i.e. ×20 objective lens and ×10 ocular lens). In the scirrhous component; the number of h-caldesmon-positive vessels was counted in all countable visual ×200 fields. Then, the mean number per field was calculated and this was taken as the arterial vessel density (AVD) in the two regions (Fig. 2e).

**Statistical analysis.** The Mann–Whitney *U*-test was used to analyze the immunohistochemical staining results. A *P*-value of <0.05 between two groups was judged to be statistically significant. Hierarchical cluster analysis of all analyzed factors was performed using TM4 MeV (http://www.tm4.org/index.html). Heat maps were generated using Microsoft Excel 2010.

## Results

**Histological features of small vaguely nodular lesions and subclassification of high-grade and low-grade of early hepatocellular carcinoma.** Of the 66 nodules, 10 were diagnosed as LGDN (15.1%), 10 as HGDN (15.1%) and 46 as eHCC (69.8%). In the eHCC nodules, no or unclear stromal invasion, suspected stromal invasion, mild distinct stromal invasion and severe

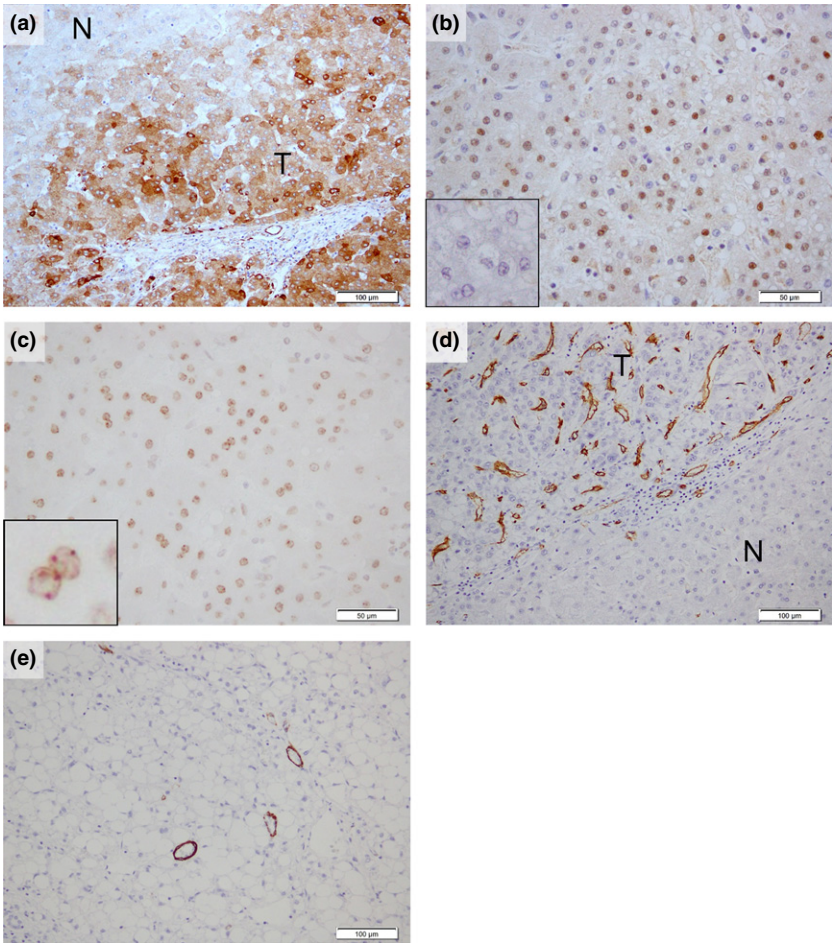


**Fig. 2.** Positive immunohistochemical expression pattern for each antibody. (a) CAP2 and (b) HSP70 showed a strong expression in the tumoral compared with the non-tumoral liver ((b) inset) and (c) Bmi-1-positive regions showed clear "dot-pattern" staining (inset). (d) Areas of CD34-positive sinusoidal vascular architectural and (e) h-caldesmon-positive unpaired vessels were seen in high-grade early hepatocellular carcinoma (HGeHCC). N, non-tumoral liver; T, tumor. Scale bars = (a),(d),(e) 100 μm; (b,c) 50 μm.

distinct stromal invasion were observed in 5, 12, 15 and 14 nodules, respectively. In addition, distinct structural atypia with the scirrhous component was found in 10 nodules. Some scirrhous components showed one regional feature per nodule, whereas other patterns showed multiple small scirrhous foci in a single nodule. Six nodules exhibited both the scirrhous component and severe distinct stromal invasion (13.0% of eHCC). Accordingly, we divided eHCC into two groups: 18 nodules (39.1% of eHCC) in which marked stromal invasion and/or the scirrhous component foci were found, and 28 nodules (60.9% of eHCC) that did not possess these features.

These two types of lesions were provisionally subclassified as high-grade early hepatocellular carcinoma (HGeHCC) and low-grade early hepatocellular carcinoma (LGeHCC) (Fig. 3a, b) according to our proposed diagnostic criteria (Fig. 4), and a further study was conducted based on this classification.

The number of nodules with large nuclei showed a tendency to increase from LGDN, to HGDN, to LGeHCC, and eventually to HGeHCC. Tumor cellularity was less than twofold compared with non-tumoral liver in all LGDN cases and was more than twofold in approximately 80% of each other nodule type. LGeHCC and HGeHCC nodules tended to be larger than DN nodules (Fig. 5a).

**Immunohistochemical features of small vaguely nodular lesions.** We further evaluated these lesions immunohistochemically. CAP2 expression-positive rates tended to increase stepwise from LGDN to HGeHCC. Although the immunohistochemical expression of CAP2 did not show a statistically significant difference between LGDN and HGDN or between HGDN and LGeHCC, there was a statistically significant difference between LGeHCC and HGeHCC ($P = 0.0145$) and between LGDN and LGeHCC ($P = 0.0034$) (Fig. 5b). In the present study, it was noted that a strong expression of CAP2 was frequently observed in tumors showing stromal invasion, hepatic vein wall invasion or a scirrhous component (Fig. 6a–c).

Both HSP70 and Bmi-1 showed statistically significant (or tendencies to have) low positive rates in DN but higher rates in eHCC. The immunohistochemical expression of HSP70 showed statistically significant differences between LGDN and LGeHCC ($P = 0.0008$) and between LGDN and HGeHCC ($P = 0.0018$) (Fig. 5c). The immunohistochemical expression of Bmi-1 showed a statistically significant difference between LGDN and LGeHCC ($P = 0.0193$) but no significant differences between other combinations (Fig. 5d).

**Vascularization of high-grade early hepatocellular carcinoma and their scirrhous component.** Vascular changes were examined in 65 nodules (excluding 1 nodule that became too small to examine during the preparation of serial sections). The area of CD34-positive sinusoid-like vascular architecture (sinusoidal capillarization) in lesions tended to gradually increase from LGDN to HGeHCC, but there were no significant differences. The scirrhous component of HGeHCC showed a very high positive rate compared with the non-scirrhous component of HGeHCC ($P = 0.0014$) (Fig. 5e). AVD was low in LGDN, HGDN and LGeHCC, with no significant differences between them. However, AVD was high in the non-scirrhous component of HGeHCC, being significantly different from that of LGeHCC ($P = 0.0054$). Moreover, the scirrhous component of HGeHCC was highlighted by a very high AVD compared with

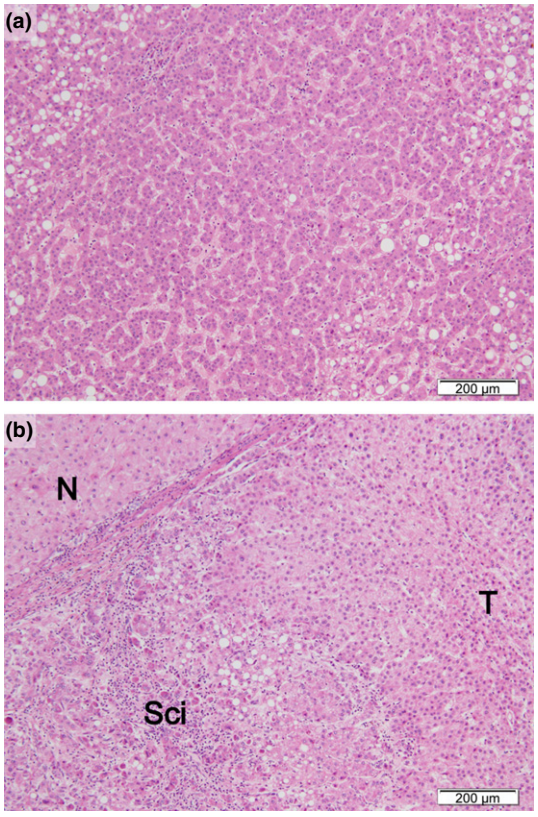


**Fig. 3.** Typical histopathological findings of low-grade early hepatocellular carcinoma (LGeHCC) and high-grade early hepatocellular carcinoma (HGeHCC). (a) LGeHCC was composed of low-grade atypical hepatocytes with high cellularity. No severe distinct stromal invasion or scirrhous component was evident. (b) HGeHCC was composed of atypical hepatocytes with a scirrhous component. N, non-tumoral liver; T, tumor; Sci, scirrhous component. (a,b) H&E stain; scale bars = 200 μm.

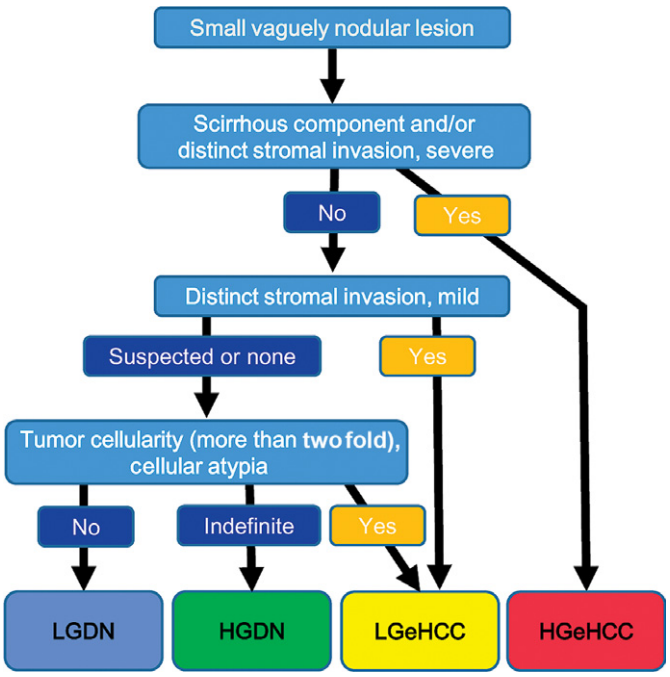


**Fig. 4.** Proposed diagnostic flow for small vaguely nodular lesions. High-grade early hepatocellular carcinoma (HGeHCC) is clearly diagnosed when there is a scirrhous component and/or severe distinct stromal invasion.

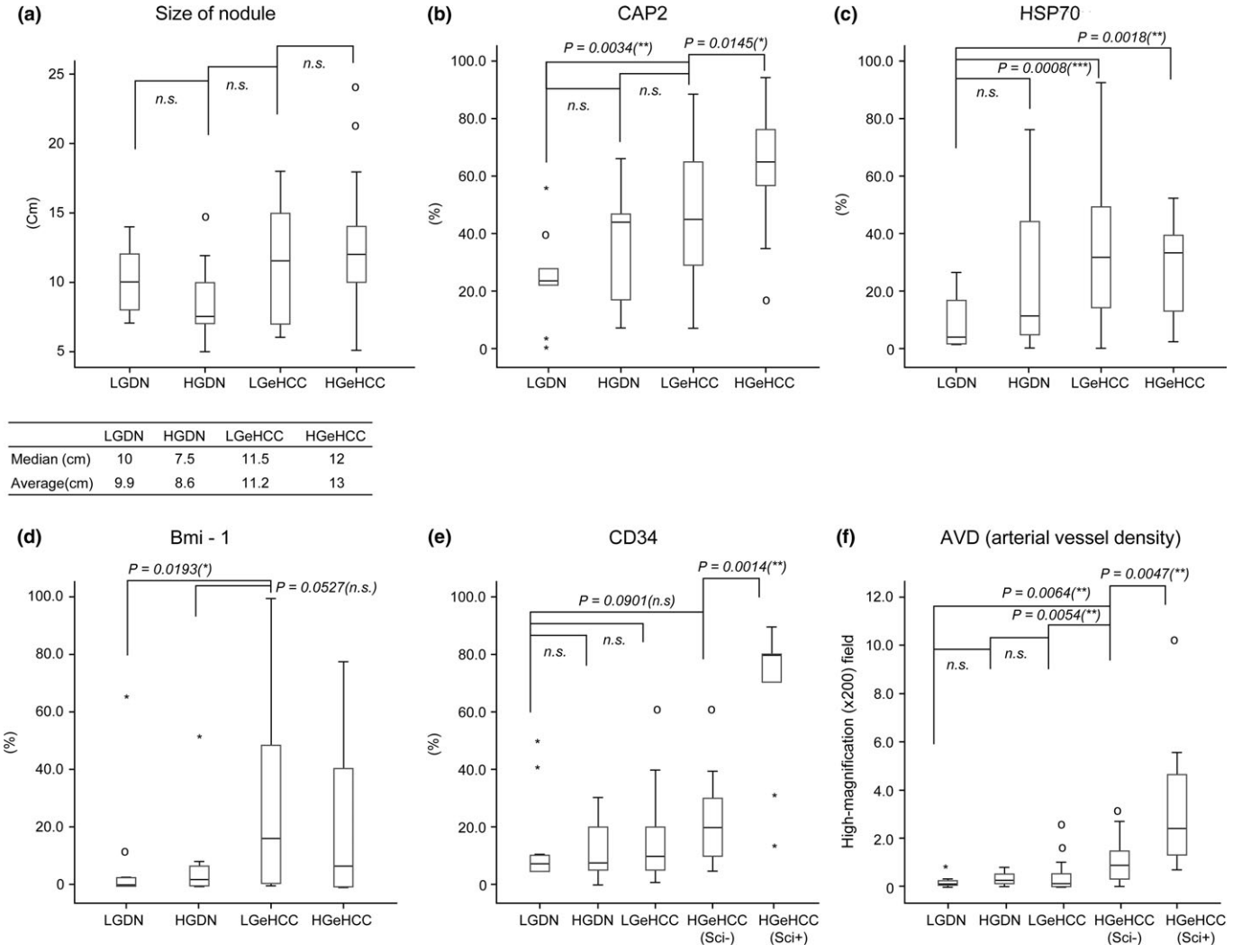


| | LGDN | HGDN | LGeHCC | HGeHCC |
|---|---|---|---|---|
| Median (cm) | 10 | 7.5 | 11.5 | 12 |
| Average(cm) | 9.9 | 8.6 | 11.2 | 13 |

**Fig. 5.** Values of histopathological factors in each type of lesion. (a) Size of nodule; the immunohistochemical expression of (b) CAP2, (c) HSP70, (d) Bmi-1 (e) and CD34; and (f) the arterial vessel density (AVD) were compared for each type of lesion. Nodule size, CAP2 expression, CD34 expression and AVD were increased for LGeHCC and/or high-grade early hepatocellular carcinoma (HGeHCC) compared with those of DN. CAP2 expression and AVD in HGeHCC were statistically higher than those in low-grade early hepatocellular carcinoma (LGeHCC) (Mann–Whitney *U*-test). CD34 expression and AVD in scirrhous components (HGeHCC Sci+) were significantly higher than those in the non-scirrhous components (HGeHCC Sci−) of HGeHCC (Mann–Whitney *U*-test). Circles, outlying data. $*P < 0.05$, $**P < 0.01$, $***P < 0.001$; n.s., not significant.

the non-scirrhous component of HGeHCC ($P = 0.0047$) (Figs 5f,6d).

**Comparison between pathological diagnoses and clustering of pathological factors in small vaguely nodular lesions.** A heat map was created for the four types of lesions (LGDN, HGDN, LGeHCC and HGeHCC) with raw data for each parameter analyzed (lesion size; tumor cellularity; size of nucleus; structure of tumor cells; extent of stromal invasion; immunohistochemical reactivity of CAP2, HSP70 and Bmi-1; the areal rate of CD34; and AVD) (Fig. S1). In addition to the original criteria defining high grade (i.e. a scirrhous component and severe stromal invasion), HGeHCC showed a tendency toward nuclear swelling and high positive expression of CAP2, CD34 and AVD compared with LGeHCC and DN.

In addition, we performed cluster analysis on each pathological factor (Fig. 7a), and this resulted in lesions being divided into three groups (Fig. 7b). Group I was composed of HGeHCC only. Group II mainly comprised HGDN and LGeHCC. Group III was mainly composed of LGDN; in fact, all LGDN appeared in group III.

## Discussion

In the present study, we divided eHCC into two subclasses, HGeHCC and LGeHCC, and conducted a detailed histological study comparing them with LGDN and HGDN. We found that HGeHCC and LGeHCC accounted for approximately 40% and 60% of eHCC, respectively. Compared with LGeHCC and DN, HGeHCC tended to have large nuclear size, high cellularity, structural atypia (including scirrhous pattern), and large tumor size together with marked stromal invasion. Immunohistochemically, both the expression of CAP2 and the areal ratio of sinusoidal capillarization were upregulated in a stepwise manner from LGDN, to HGDN, to LGeHCC, and eventually to HGeHCC. In contrast, AVD was almost unchanged in LGeHCC compared with DN, whereas AVD in HGeHCC was

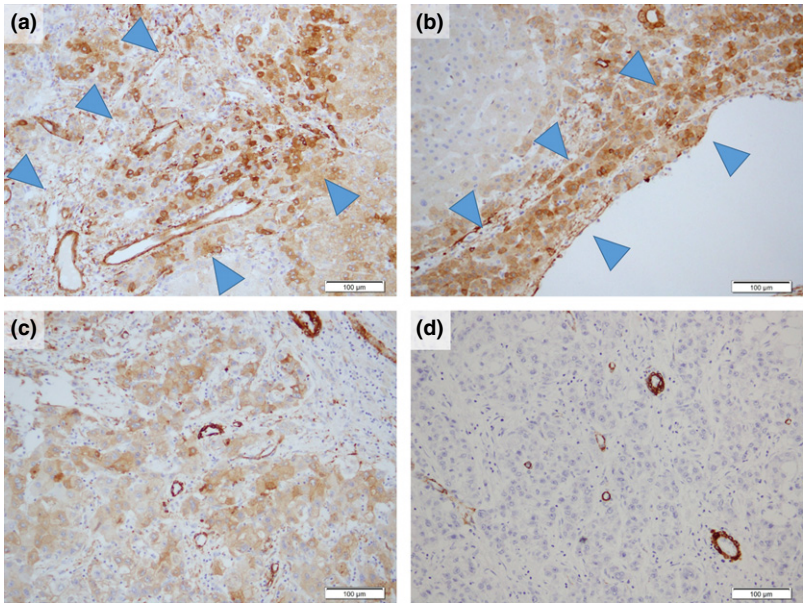


**Fig. 6.** Immunohistochemical findings of CAP2 and h-caldesmon in high-grade early hepatocellular carcinoma (HGeHCC). The strong expression of CAP2 was frequently observed in tumors showing (a) portal area invasion (arrowheads, the same area of Fig. 2b), (b) hepatic vein wall invasion (arrowheads, the same area of Fig. 2d and e) and (c) scirrhous component. (d) Areas of scirrhous component in HGeHCC were highlighted by very high levels of arterial vessel density (AVD), as indicated by the h-caldesmon-positive vessels. Scale bars = 100 μm.

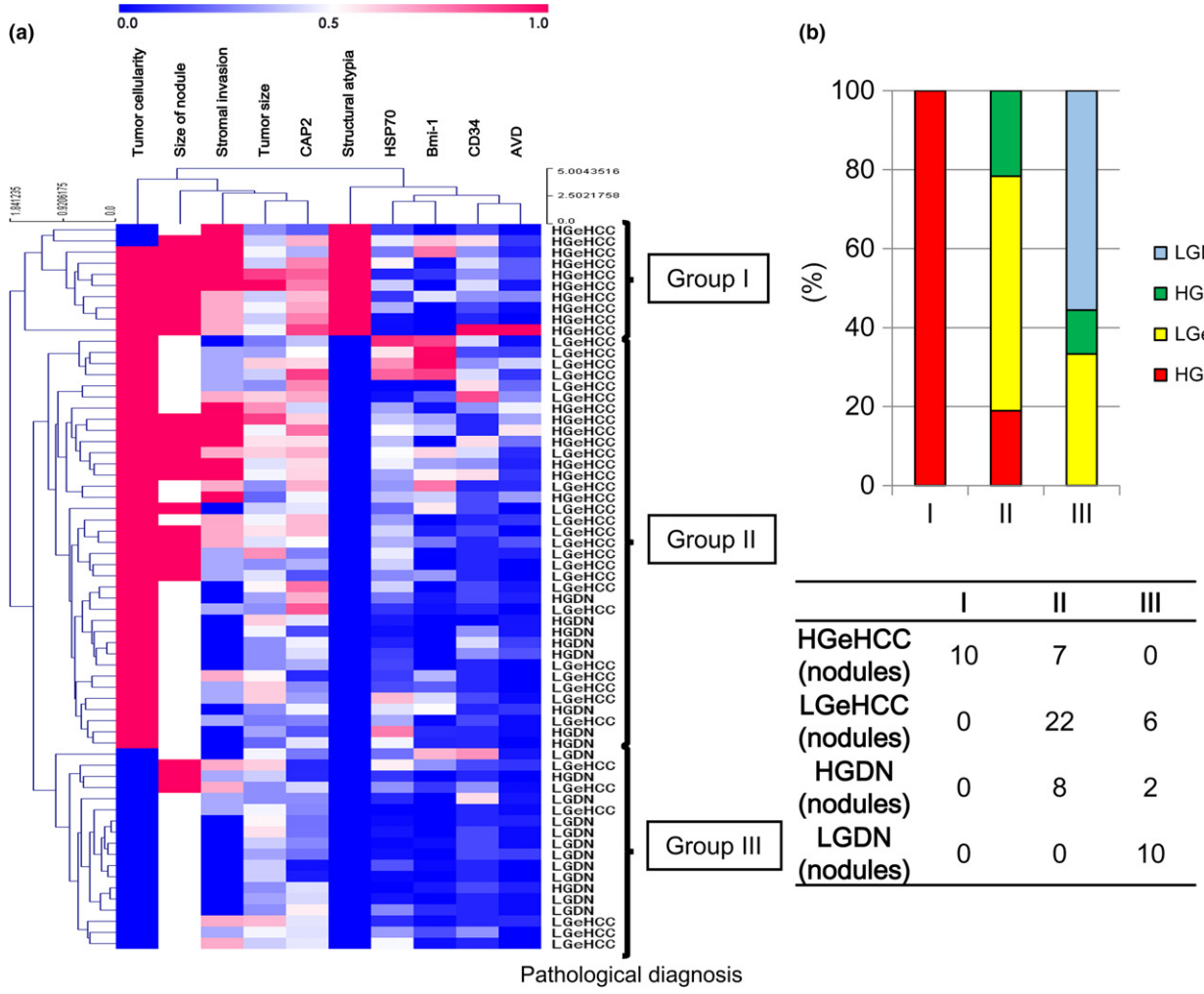


| | I | II | III |
|---|---|---|---|
| HGeHCC (nodules) | 10 | 7 | 0 |
| LGeHCC (nodules) | 0 | 22 | 6 |
| HGDN (nodules) | 0 | 8 | 2 |
| LGDN (nodules) | 0 | 0 | 10 |

**Fig. 7.** Cluster analysis of pathological factors. (a) The lesions were clearly divided into three groups based on pathological factors. (b) Group I was composed of high-grade early hepatocellular carcinoma (HGeHCC) only. Group II mainly comprised high-grade dysplastic nodules (HGDN) and low-grade early hepatocellular carcinoma (LGeHCC). Group III was mainly composed of low-grade dysplastic nodules (LGDN); all LGDN were included in group III.

higher. Statistically significant differences between LGeHCC and HGeHCC were found for CAP2 expression and AVD. Moreover, vascularization in the scirrhous component of HGeHCC was different from that in the non-scirrhous component of HGeHCC. Based on the above findings, we considered that HGeHCC is histopathologically distinct from LGeHCC.

In a previous study using an oligonucleotide array, we found that CAP2 was upregulated in early HCC,[11] and high immunohistochemical expression of CAP2 was shown in HCC with increased malignant potential, such as those with poor tumor differentiation, vascular invasion and intrahepatic metastasis.[13] Therefore, a significant overexpression of CAP2 in HGeHCC likely indicated increased malignant potential of the lesion. Moreover, hypervascularization in small lesions in chronic liver disease is thought as an indicator of increased malignant potential. AVD and the area with sinusoidal capillarization in HGeHCC were high in comparison with LGeHCC and DN. Indeed, during follow up, small vaguely nodular lesions generally show poor arterial blood flow on hemodynamics imaging;[15,16] however, approximately 10–40% of such lesions may become hypervascular tumors within a year.[17–19] It has also been reported that tumor cells of nodular lesions larger than 15 mm, which is similar to the 13 mm mean size of HGeHCC, actively proliferated with the emergence of unpaired arteries.[20] We consider that HGeHCC has distinct histological malignant features that may represent a transitional stage to advanced HCC.

While HSP70 and Bmi-1 are not correlated with the malignant potential of HCC, they are valuable for differentiation between DN and eHCC, as reported previously.[11,14] We found no significant differences in the expressions of HSP70 and Bmi-1 between LGeHCC and HGeHCC, although Bmi-1 expression tended to decrease slightly. This is in agreement with our previous observation of a higher expression of Bmi-1 in well-differentiated HCC (including early HCC) than in moderate and poorly differentiated HCC.[14]

The scirrhous pattern or marked stromal invasion was frequently observed in eHCC. These are generally characteristics that support a diagnosis of cancer; however, it should be noted that these features are not pronounced in advanced HCC. Because we observed marked vascularization in the scirrhous component, we believe that the scirrhous component may be an indicator of the high neovascularization capabilities of HGeHCC. Marked stromal invasion also may be an indicator of high invasiveness, resulting in portal vein invasion and intrahepatic metastasis. Therefore, we consider that the criteria presented here for classifying HGeHCC (i.e. the presence of foci with a scirrhous component and/or marked stromal invasion) are reasonable.

To assess the validity of our pathological diagnosis of nodules, the pathological factors that we examined were analyzed using cluster analysis. The clustering of pathological factors and the pathological diagnosis (LGDN, HGDN, LGeHCC and HGeHCC) were compared. Interestingly, cluster analysis showed that lesions were divided into three groups. Group I was made up entirely of HGeHCC, and 10 of the 17 HGeHCC nodules (59%) were subclassified into this group. Group II mainly comprised HGDN and LGeHCC, and group III was dominated by LGDN (all 10 LGDN were included in group III). These results further confirmed the distinct features of HGeHCC that we classified histopathologically. The scirrhous component is one of the key histopathological factors between group I and group II. Group II may indicate that the pathological features of LGeHCC (i.e. eHCC excluding HGeHCC) may overlap with those of HGDN. The above findings suggest that HGDN and LGeHCC may be considered "borderline" lesions, whereas HGeHCC is a distinct malignant tumor. In addition, immunohistochemical expression of CAP2 and CD34, and AVD may assist diagnosis of HGeHCC, even if marked stromal invasion or a microscopic scirrhous component is not evident in biopsy specimens. However, further analysis is necessary using a large series of cases with the inclusion of biopsy specimens.

In conclusion, we investigated detailed histological and immunohistochemical features of small vaguely nodular lesions. Our results indicated that from the perspective of histopathology, immunohistology and changes in vascularization, approximately 40% of eHCC cases belonged to a distinct, highly malignant tumor group that we subclassified as HGeHCC. In addition, we believe that HGeHCC may already be a transitional stage to advanced HCC. We consider that our grading classification system may be valuable for evaluating treatment strategies for eHCC with a size of approximately 2 cm.

## Acknowledgments

We sincerely thank Mr Hiroshi Suzuki, Dr Yutaka Kurebayashi and Dr Ken Yamazaki for their kind advice on immunohistochemistry and statistics.

## Disclosure Statement

The other authors have no conflict of interest to declare.

## References

1 Takayama T, Makuuchi M, Hirohashi S *et al.* Malignant transformation of adenomatous hyperplasia to hepatocellular carcinoma. *Lancet* 1990; **336**: 1150–3.
2 Sakamoto M, Hirohashi S, Shimosato Y. Early stages of multistep hepatocarcinogenesis: adenomatous hyperplasia and early hepatocellular carcinoma. *Hum Pathol* 1991; **22**: 172–8.
3 Sakamoto M. Pathology of early hepatocellular carcinoma. *Hepatol Res* 2007; **37**(Suppl 2): S135–8.
4 Sakamoto M, Effendi K, Masugi Y. Molecular diagnosis of multistage hepatocarcinogenesis. *Jpn J Clin Oncol* 2010; **40**: 891–6.
5 International Consensus Group for Hepatocellular Neoplasia. Pathologic diagnosis of early hepatocellular carcinoma: a report of the international consensus group for hepatocellular neoplasia. *Hepatology* 2009; **49**: 658–64.
6 Theise ND, Curado MP, Franceschi S *et al.* Hepatocellular carcinoma. In: Bosman E, *et al.*, eds. *WHO Classification of Tumors of the Digestive System*, 4th edn. Lyon: IARC, 2010; 205–16.
7 Kitao A, Matsui O, Yoneda N *et al.* The uptake transporter OATP8 expression decreases during multistep hepatocarcinogenesis: correlation with gadoxetic acid enhanced MR imaging. *Eur Radiol* 2011; **21**: 2056–66.
8 Kitao A, Zen Y, Matsui O, Gabata T, Nakanuma Y. Hepatocarcinogenesis: multistep changes of drainage vessels at CT during arterial portography and hepatic arteriography–radiologic-pathologic correlation. *Radiology* 2009; **252**: 605–14.
9 Sakamoto M, Hirohashi S. Natural history and prognosis of adenomatous hyperplasia and early hepatocellular carcinoma: multi-institutional analysis of 53 nodules followed up for more than 6 months and 141 patients with single early hepatocellular carcinoma treated by surgical resection or percutaneous ethanol injection. *Jpn J Clin Oncol* 1998; **28**: 604–8.
10 Ueda K, Terada T, Nakanuma Y, Matsui O. Vascular supply in adenomatous hyperplasia of the liver and hepatocellular carcinoma: a morphometric study. *Hum Pathol* 1992; **23**: 619–26.
11 Chuma M, Sakamoto M, Yamazaki K *et al.* Expression profiling in multistage hepatocarcinogenesis: identification of HSP70 as a molecular marker of early hepatocellular carcinoma. *Hepatology* 2003; **37**: 198–207.

12 Di Tommaso L, Franchi G, Park YN *et al.* Diagnostic value of HSP70, glypican 3, and glutamine synthetase in hepatocellular nodules in cirrhosis. *Hepatology* 2007; **45**: 725–34.
13 Shibata R, Mori T, Du W *et al.* Overexpression of cyclase-associated protein 2 in multistage hepatocarcinogenesis. *Clin Cancer Res* 2006; **12**: 5363–8.
14 Effendi K, Mori T, Komuta M *et al.* Bmi-1 gene is upregulated in early-stage hepatocellular carcinoma and correlates with ATP-binding cassette transporter B1 expression. *Cancer Sci* 2010; **101**: 666–72.
15 Matsui O, Kadoya M, Kameyama T *et al.* Benign and malignant nodules in cirrhotic livers: distinction based on blood supply. *Radiology* 1991; **178**: 493–7.
16 Hayashi M, Matsui O, Ueda K *et al.* Correlation between the blood supply and grade of malignancy of hepatocellular nodules associated with liver cirrhosis: evaluation by CT during intraarterial injection of contrast medium. *AJR Am J Roentgenol* 1999; **172**: 969–76.
17 Kumada T, Toyoda H, Tada T *et al.* Evolution of hypointense hepatocellular nodules observed only in the hepatobiliary phase of gadoxetate disodium-enhanced MRI. *AJR Am J Roentgenol* 2011; **197**: 58–63.
18 Motosugi U, Ichikawa T, Sano K *et al.* Outcome of hypovascular hepatic nodules revealing no gadoxetic acid uptake in patients with chronic liver disease. *J Magn Reson Imaging* 2011; **34**: 88–94.
19 Kobayashi S, Matsui O, Gabata T *et al.* Gadolinium ethoxybenzyl diethylenetriamine pentaacetic acid-enhanced magnetic resonance imaging findings of borderline lesions at high risk for progression to hypervascular classic hepatocellular carcinoma. *J Comput Assist Tomogr* 2011; **35**: 181–6.
20 Kojiro M. Angioarchitecture of hepatocellular carcinoma. In: Kojiro M, ed. *Pathology of Hepatocellular Carcinoma*. Oxford: Blackwell Publishing, 2006; 63–76.

## Supporting Information

Additional supporting information may be found in the online version of this article:

**Fig. S1.** Heat map of the raw analyzed parameters in each lesion.

**Table S1.** Patient background summary.